Advanced Ceramics Progress: Vol. 11, No. 1, (Winter 2025) 19-27

Materials and Energy Research Center
MERC

Contents lists available at ACERP

Advanced Ceramics Progress

Journal Homepage: www.acerp.ir

Original Research Article

Exploring the Antibacterial Potential of Zinc Sulfide/Chitosan Nanocomposites

Mohammad Mahdi Hosseinieh Farahani [a], Maryam Hajiebrahimi [b], Amir Hossein Afzali [a], Danial Moradi [a], Sanaz Alamdari [c]*, Omid Mirzaee [d]*

[a] *BSc Student, Faculty of Materials and Metallurgical Engineering, Semnan University, Semnan, Iran.*
[b] *Research Assistant, Faculty of Materials and Metallurgical Engineering, Semnan University, Semnan, Iran.*
[c] *Assistant Professor, Department of Nanotechnology, Faculty of New Sciences and Technologies, Semnan University, Semnan, Iran.*
[d] *Professor, Faculty of Materials & Metallurgical Engineering, Semnan University, Semnan, Iran.*

* Corresponding Author Email: o_mirzaee@semnan.ac.ir (O. Mirzaee); s.alamdari@semnan.ac.ir (S. Alamdari) URL: https://www.acerp.ir/article_225611.html

ARTICLE INFO

Article History:
Received 30 October 2024
Received in revised form 30 November 2024
Accepted 15 July 2025

Keywords:
Nanocomposite,
Zinc Sulfide,
Chitosan,
Nanoparticle,
Antibacterial Activity

ABSTRACT

Bacterial infections are a rising concern, and nanomaterials offer promising solutions to combat them. The synthesis and antibacterial characteristics of zinc sulfide/chitosan nanocomposite were investigated to solve this critical issue, paving the way for new possibilities in this filed. The manufacturing and analysis of these nanocomposites were also studied based on some imaging methods such as XRD, FTIR, FESEM, EDX elemental mapping, and antibacterial (a colony count method). The results from XRD indicated that chitosan and hexagonal ZnS crystals with the average size of 30-40 nm formed ZnS/CS nanoparticles. The FTIR spectrum revealed nanoparticle groups and bonding which were indicative of synthesis and stability. Additionally, FESEM imaging demonstrated the surface shape of the nanocomposite with a particle size distribution of 212-nm, and EDX confirmed its components and composition. Antibacterial effectiveness against Gram-positive (Staphylococcus aureus) and Gram-negative (Escherichia coli) bacteria was also evaluated. ZnS nanoparticles and ZnS/CS nanocomposite were found to be more potent than CS and ZnS alone. These findings show that the produced samples may provide insights into prospective paths for fighting bacterial infections and enhancing biomedical technologies.

https://doi.org/10.30501/acp.2025.486319.1164

1. INTRODUCTION

Nanomaterials have played a significant role in advancing materials research over the past two decades. These materials are characterized by some unique physical and chemical properties as well as high surface area/volume, compared with bulk counterparts (Mekuye et al, 2023; Alamdari et al, 2022a). In this respect, there were some advancements in synthesis including the development of new compounds, minimization of nanomaterial sizes, and introduction of innovative morphologies through assembly or templating techniques. This technology involves materials whose structures offer significantly improved physicochemical and biological properties, along with unique phenomena and functionalities due to their nanoscale dimensions (Paula et al, 2017). Nanoparticles are recognized as controlled or manipulated entities on the atomic scale, ranging from 1 to 100 nanometers. Their size-related properties exhibit significant differences compared to bulk materials (Hassan, 2020). Owing to their diminutive size, NPs have larger structures than those of their counterparts. This unique property enables potential applications across various domains, including biosensors, nanomedicine, and bionanotechnology (Carstens et al, 2021). Antibiotic-resistant bacteria have emerged and grown as a result of their widespread

Please cite this article as: Hosseinieh Farahani, M. M. , Hajiebrahimi, M., Afzali, A. H., Moradi, D., Alamdari, S., & Mirzaee, O. (2025). Exploring the Antibacterial Potential of Zinc Sulfide/Chitosan Nanocomposites, *Advanced Ceramics Progress*, 11(1), 19-27. https://doi.org/10.30501/acp.2025.486319.1164

overuse, posing serious health challenges. In healthcare and production sectors, substances are essential to fight bacterial infections and ensure the product longevity (Frieri et al, 2017). While extensive study has been conducted on metal nanoparticles, semiconducting nanomaterials offer even greater potential in terms of their application, functionality, and adaptability. ZnS is an inorganic semiconductor nanomaterial that is particularly attractive owing to its unique optical, biological, and antimicrobial properties, as well as its non-toxicity (Singh et al, 2022). Zinc sulfide nanoparticles, synthesized through coprecipitation technique, are receiving recognition for their promising role in effectively combating microbes. Nano-sized ZnS demonstrates diverse morphologies and exhibits considerable antibacterial activity against a broad range of bacterial species investigated by numerous researchers (Duwarah et al, 2023). ZnS is presently under investigation as an antibacterial agent in both microscale and nanoscale formulations. ZnS demonstrates notable antimicrobial properties when minimizing its particle size to the nanometer scale. At this size, nano-sized ZnS interact with bacterial surfaces and/or penetrate the bacterial core, triggering some specific bactericidal mechanisms (Badabagni et al, 2023). The shells of marine crustaceans are used to produce a biopolymer called chitosan. However, chitosan which is commonly sold in stores is made by deacetylating chitin, a naturally occurring biopolymer that may be found in lobster, crab, and coral shrimp. The molecular chain length, content, and sequencing of the N-acetyl glucosamine and D-glucosamine units that make up chitosan are all randomly distributed (Alamdari et al, 2022b). The integration of metallic nanoparticles into chitosan significantly enhances its applicability across various domains, including catalysis and environmental sectors. The current paper primarily focuses on antimicrobial activity (Khoerunnisa et al, 2023). Chitosan-stabilized metallic nanoparticles have garnered significant attention from researchers since chitosan exhibits antimicrobial activity both independently and in conjunction with attached metal nanoparticles. It demonstrates outstanding antimicrobial properties. Researchers have proposed various mechanisms underlying the antimicrobial properties of chitosan, one of which indicates that chitosan serves as an effective chelating agent that binds to the metals within the microbial cell upon contact, disrupting the cell function and leading to bacterial death (Ameh et al, 2023). Bionanocomposites that mix biopolymers with nanoparticles offer unique characteristics and applications. These nanocomposites have gained popularity owing to their ability to fight multiple-drug resistant bacteria. Nanotechnology plays a crucial role in customizing the attributes of nanocomposites, enabling management of nanoparticle size, shape, and placement in the biopolymer structure (Pires et al, 2023). A novel approach that integrates the properties of both materials is formed by combining chitosan with zinc oxide nanoparticles to produce zinc oxide/chitosan nanocomposites. The co-precipitation approach has shown potential as a means of producing these nanocomposites. Incorporation of ZnS nanoparticles into chitosan matrices using the co-precipitation approach significantly enhances their characteristics. Although chitosan and ZnS both have antibacterial activities against both Gram-positive and Gram-negative bacteria on their own, they commonly work together as a nanocomposite, making them far more powerful than either one alone (Mustafa et al, 2023). The higher antibiotic activity comes from chitosan and ZnS nanoparticles working together in more than one way, which makes their surface area and stability bigger. Nanocomposites made of zinc and chitosan have widespread applications, such as in health devices, water treatment, and food packaging, etc., owing to their better quality, changeability, and biocompatibility (Kang et al, 2023). This study primarily aims to investigate the structure and characteristics of a hybrid ZnS/CS. The synthesized composite was tested against two different germs to examine its antimicrobial efficacy. ZnS/CS composites are being explored for their potential to inhibit the growth of harmful bacteria, with promising applications across various fields.

2. MATERIALS AND METHODS

2.1. REAGENTS

All of the chemical solutions retained their scientific grade and do not require further cleaning. We sourced to 99.9% pure zinc acetate dihydrate (Zn $(CH_3CO_2)_2{\cdot}2H_2O$), sodium sulfide ($Na_2S.9H_2O$), acetic acid, and tripolyphosphate (TPP) from Sigma-Aldrich. Ethanol and deionized water were used to make water-based remedies. The shrimp used in this study were sourced from the coastal waters of Bandar Abbas, located in the Hormozgan Province, Persian Gulf. The process of converting finely ground chitin from shrimp and crab shells into chitosan involves several steps: demineralization, discoloration, deproteinization, and deacetylation. The final chitosan exhibits a deacetylation level ranging from 75% to 85%. The standard strains for the antimicrobial tests were provided by the Medical University of Tehran in Iran.

2.2. SYNTHESIS OF ZnS NPs

The co-precipitation method was employed to synthesize zinc sulfide nanoparticles, referred to as ZnS NPs. A magnetic stirrer was employed to dissolve 3 grams of sodium sulfide and 5 grams of zinc acetate in 50 cc of distilled water for a duration of 30 minutes each. The sodium sulfide solution was subsequently added dropwise to the zinc acetate solution using a separating funnel in a systematic manner. The combination of zinc acetate and sodium sulfide solutions resulted in the formation of a white precipitate. Subsequently, the resultant solid was washed, followed by centrifugation

three times at 4,000 rpm to facilitate the separation of its components, and then it was dried at 90 °C. The sample underwent calcination at 800 °C for 1 hour in the penultimate step, hence production of zinc sulfide powder.

2.3. SYNTHESIS OF ZnS/CS NANOCOMPOSITE

In this study, 10 milliliters of distilled water and acetic acid (CH_3COOH) at a concentration of 1% by volume were used to dissolve 0.75 grams of bought chitosan. The mixture was stirred with a magnetic stirrer set at 250 revolutions per minute for 3 hours at room temperature. Next, 0.25 grams of zinc sulfide were added to the mixture and mixed using an ultrasound-assisted emulsification method at a frequency of 20 kHz for twenty minutes. Then, ten milliliters of distilled water were used to construct a solution containing 0.002% TPP, which is equivalent to 0.04 weight percent by volume. Subsequently, the solution was carefully introduced into the homogeneous emulsion while maintaining stirring for a duration of 30 minutes. The resulting nanopowders (NPs) were finally collected through centrifugation at 4000 rpm following a drying process at 80 °C.

Figure 1 illustrates the processes involved in the production of ZnS nanoparticles and a ZnS/CS nanocomposite.

2.4. CHARACTERIZATION

Characterization involves analyzing and detailing a traits, characteristics, and features of a material or sample. Imaging methods such as XRD, FTIR, FESEM, and EDX mapping were used to characterize the produced sample. An X-ray diffractometer (Bruker D8-Advance) and Cu K± radiation (λ = 1.5406 Å) were used to examine the crystal structure of the nanopowder. Additionally, a Perkin-Elmer Model 1800 spectrometer was used to get the Fourier transform infrared spectra of the ZnS/CS nanocomposites. A Field Emission Scanning Electron Microscope (FESEM), specifically the MIRA3TESCAN-XMU model, was also utilized to study the morphology of the synthesized powder and composite.

3. RESULTS AND DISCUSSION

3.1. X-RAY DIFFRACTION (XRD)

X-ray diffraction analysis is the main technique for determining the structural characteristics of the samples. The XRD patterns of Chitosan, ZnS, and a nanocomposite of ZnS and Chitosan are shown in Figure 2. The amorphous nature of chitosan is confirmed by its big peaks around 2θ=10° and 2θ=20° in the XRD pattern. Black stars indicate a big peak between 10 and 20 degrees, which is a typical characteristic of chitosan. This peak is indicative of the semi-crystalline structure of chitosan, confirming that it contains both crystalline and amorphous parts (Valinezhad et al, 2023).

The middle curve reveals prominent and well-defined peaks, indicating a high degree of crystallinity of ZnS. The following peaks are associated with different ZnS crystal planes: (100), (002), (101), (110), (103), (200), (112), (201), (202), (203), and (210). Their presence confirms that the ZnS crystal structure is hexagonal wurtzite (Hajiebrahimi et al, 2024; Afzali et al, 2024).

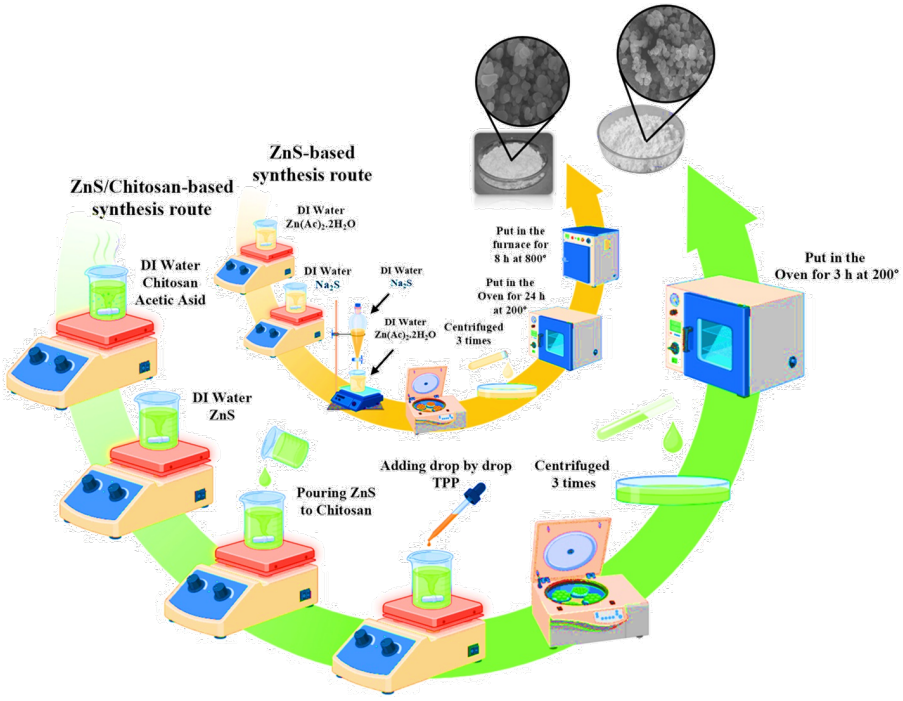

Figure 1. Brief schematic of the experimental works

This structure aligns with the standard diffraction pattern provided in the reference card (JCPDS card no. 96-901-3413), which has crystal lattice constants of a = 0.382 and c = 0.626. In addition, the patterns of both ZnS and chitosan can be seen on the top curve. Sharp peaks marked by pink stars represent the crystalline nature of ZnS in the composite. The two broad chitosan peaks are also visible, although they are overshadowed by the greater diffraction from the ZnS crystals. It seems that the ZnS has been well incorporated into the chitosan matrix since the ZnS peaks are more intense than the chitosan peak. To find the crystal size of every nanoparticle (NP) sample, Scherrer's Equation (Eq. 1) was used. This method determines the average crystal size from three peaks with the highest intensities, using X-ray diffraction angle (θ) and breadth at half the height of the principal peak (β). The following formula is used to determine the size of a crystallite ('D') in nanometers, where 'K' is the average crystallite's shape factor (usually 0.9) (Hajiebrahimi et al, 2025; Hajiebrahimi et al, 2022; Moradi et al, 2024):

$$D = \frac{K\lambda}{\beta \cos\theta} \quad (1)$$

The average particle size for pure ZnS and ZnS/Chitosan nanocomposite samples were calculated as 38.56 nm and 32.95 nm, respectively. Other structural parameters of samples are reported in Table 1.

3.2. FTIR

The FTIR spectra of three samples—CS, ZnS, and ZnS/CS—are given in Figure 3.

The frequencies of all analyzed vibrational bands are presented in Tables 2 and 3. The peak at 3427 cm^{-1} in the FTIR spectra of chitosan confirms the presence of hydroxyl and amine groups (O-H and N-H stretching). The peak at 2880 cm^{-1} (CH_2) corresponds to the stretching vibrations of methylene groups in the compound. Carbonyl groups, most likely caused by acetylation in chitosan, are also identified by C=O stretching at 1609 cm^{-1}. In addition to the C-N stretching peak at 1074 cm^{-1}, which validates the existence of the chitosan-characteristic C-N bond, an additional NH_2 stretching peak at 1390 cm^{-1} indicates the presence of amine groups (Alamdari et al, 2025). The prominent peak in the middle curve of ZnS FTIR spectra, which corresponds to O-H stretching at 3438 cm^{-1}, is related to the surface hydroxyl groups or adsorbed water. Hydrocarbons (2904 cm^{-1}) at the carbon-hydrogen bond suggest confirms the application of organic contaminants or surfactants during production. The C=O stretching peak at 1629 cm^{-1} shows that there are carbonyl groups. It looks like the organic molecules used in the process have C-N bonds based on the C-N stretching peak at 1170 cm^{-1}. The Zn-S stretching peak at 617 cm^{-1} shows that zinc sulfide bonds are present (Aqeel et al, 2020). The FTIR spectra of the ZnS/CS hybrid exhibit stretching of the O-H and N-H bonds around 3427 cm^{-1}. This structure is comparable to that of chitosan and reveals the presence of hydroxyl and amine groups. The methylene groups found in chitosan are identical to the CH_2 hydrocarbon signal at 2880 cm^{-1}.

TABLE 1. Measurements of crystallite size of samples.

Sample	Peak position (°)	FWHM	D (nm)
ZnS	28.5646 47.5511 56.3899	0.1771 0.2362 0.2952	38.56
ZnS/CS	28.6421 47.6255 56.3502	0.2362 0.2952 0.2952	32.95

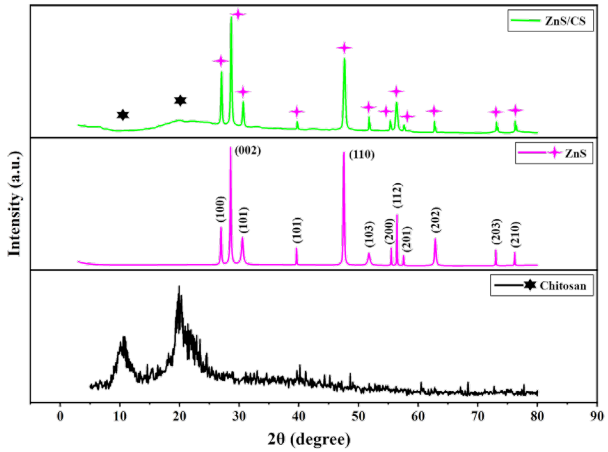

Figure 2. XRD patterns of pure ZnS, CS nanopowders, and ZnS/CS nanocomposite.

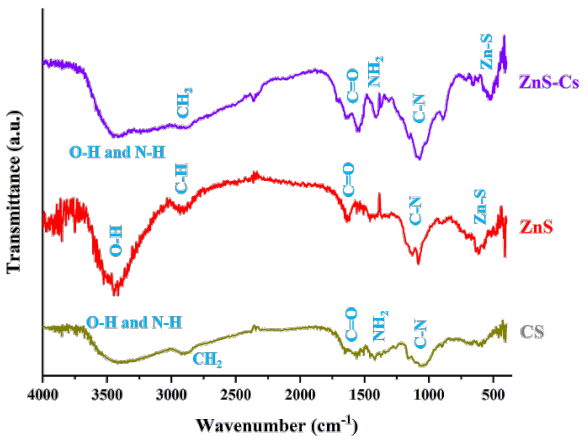

Figure 3. FT-IR absorption spectra of pure ZnS, CS NPs, and ZnS/CS nanocomposite.

TABLE 2. FTIR DATA of different vibrational stretching of ZnS nanoparticles.

Wave number (cm^{-1})	Vibrational ranges
ZnS	
3438	O-H Stretching
2904	C-H Hydrocarbon
1629	C=O Stretching
1170	C-N Stretching
617	Zn-S Stretching

TABLE 3. FTIR DATA of different vibrational stretching of ZnS/CS nanoparticles.

Wave number (cm^{-1})	Vibrational ranges
ZnS/CS	
3427	O-H and N-H Stretching
2880	CH_2 Hydrocarbon
1609	C=O Stretching
1390	NH_2 Stretching
1074	C-N Stretching
518	Zn-S Stretching

The presence of amine groups is confirmed by the appearance of peaks at 1609 cm^{-1} for carbonyl groups and 1390 cm^{-1} for NH_2 components. In addition, the presence of signature chitosan peaks in the ZnS/CS nanocomposite further proves the effective incorporation of chitosan with ZnS while the C-N stretching (1074 cm^{-1}) peak verifies the presence of C-N bonds. Further, the Zn-S stretching (518 cm^{-1}) peak is indicative of zinc sulfide bonds, slightly shifted relative to pure ZnS (Aboelwafa et al, 2021).

3.3. FESEM IMAGES

Figure 4 depicts the morphology and particle size distribution of three samples: (a) chitosan, (b) ZnS, and (c) ZnS/chitosan. These samples will be discussed in more detail in the following paragraphs. As observed in Figure 4(a), the surface morphology of the Chitosan sample is rough and fibrous, containing pores and microfibrils that are visible. Nanoparticles with a combination of spherical and hexagonal structures with a size range of 100-200 nm are generated (Alamdari et al, 2023). As shown in Figure 4 (b, c) and the FESEM images, ZnS NPs are distributed throughout the chitosan. These qualities are combined in the ZnS/Chitosan nanocomposite, thus improving the material properties of chitosan by combining the nanoscale features of ZnS with those of the chitosan matrix (Aqeel et al, 2020). According to the histogram examination of the particle size distribution, ZnS NPs have an average diameter of about 155 nm while the ZnS/CS nanocomposite has an average diameter of around 210 nm. Figure 5 shows that the produced nanocomposite samples contain C, O, Zn, and S, as determined by elemental mapping using energy-Dispersive X-ray Spectroscopy (EDS).

3.4. ANTIBACTERIAL ACTIVITY

Using Control, Chitosan, ZnS, and ZnS/Chitosan nanocomposite treatments, Figure 6. shows the antibacterial test against Staphylococcus aureus (ATCC 25923) and Escherichia coli (ATCC 25922), as well as other microorganisms. The outcomes are presented for two settings (inside and out), at one-hour, three-hour, and six-hour intervals. Figure 6 and Table 4 display the findings of the tests conducted to determine the antibacterial effect of CS, ZnS NPs, and the ZnS/Chitosan nanocomposite. The samples without nanoparticles served as the control group. The bacteria cultures were grown and maintained using trypticase soy agar. The bacterial suspension was adjusted to achieve a density equivalent to 0.5 McFarland standards, which is 1.5×10^1 CFU/mL (Farahani et al, 2024). According to Figure 6 and Table 4, the Chitosan sample underwent a small decrease in S. aureus, with a reduction of less than 5% after 1 hour, which persisted at 3 and 6 hours. ZnS demonstrated a negligible decrease at 1 hour which increased up to 40% at 3 hours and remained constant at 6 hours. ZnS/CS exhibited 10% antibacterial activity at 1 hour, which increased up to 60% at 3 hours and maintained 60% at 6 hours, demonstrating the maximum antibacterial activity. Chitosan consistently contained less than 5% E. coli, indicating weak antibacterial action. Regularly having less than 5% E. coli, chitosan showed very little antibacterial action. ZnS exhibited weak antibacterial action, with reductions consistently below 5%. In contrast, the ZnS/CS nanocomposite displayed the highest activity, achieving a 20% reduction at 1 hour, 3 hours, and 6 hours. Combining ZnS nanoparticles with chitosan synergistically enhanced the antibacterial activity of the ZnS/CS nanocomposite. ZnS nanoparticles are antimicrobial because they create ROS, which damage bacterial cells (Kusrini et al, 2023). Chitosan breaks bacteria cell membranes and makes ZnS nanoparticles more stable and dispersible, improving their antibacterial properties. When combined in a nanocomposite, ZnS and Chitosan synergically enhance the overall antibacterial activity by increasing bacterial cell contact, stabilizing ZnS nanoparticles and improving their distribution (Farahani et al, 2024).

This study indicated that Gram-positive Staphylococcus aureus was more resistant than Gram-negative E. coli. The thick peptidoglycan cell walls of Gram-positive bacteria protect them from outside influences while keeping their structure stable. Gram-negative bacteria have a thinner peptidoglycan layer; however, their outer membrane has lipopolysaccharides, which makes them easier to kill with antibiotics. Different levels of resistance are partly attributed to how the cell walls are built. For example, Gram-positive Staphylococcus aureus and Gram-negative Escherichia coli exhibit different levels of resistance to antibiotics (Ali et al, 2021; Budea et al, 2023; Zannat et al, 2023).

The antibacterial mechanism of action of ZnS/Chitosan nanocomposite is illustrated in Figure 7.

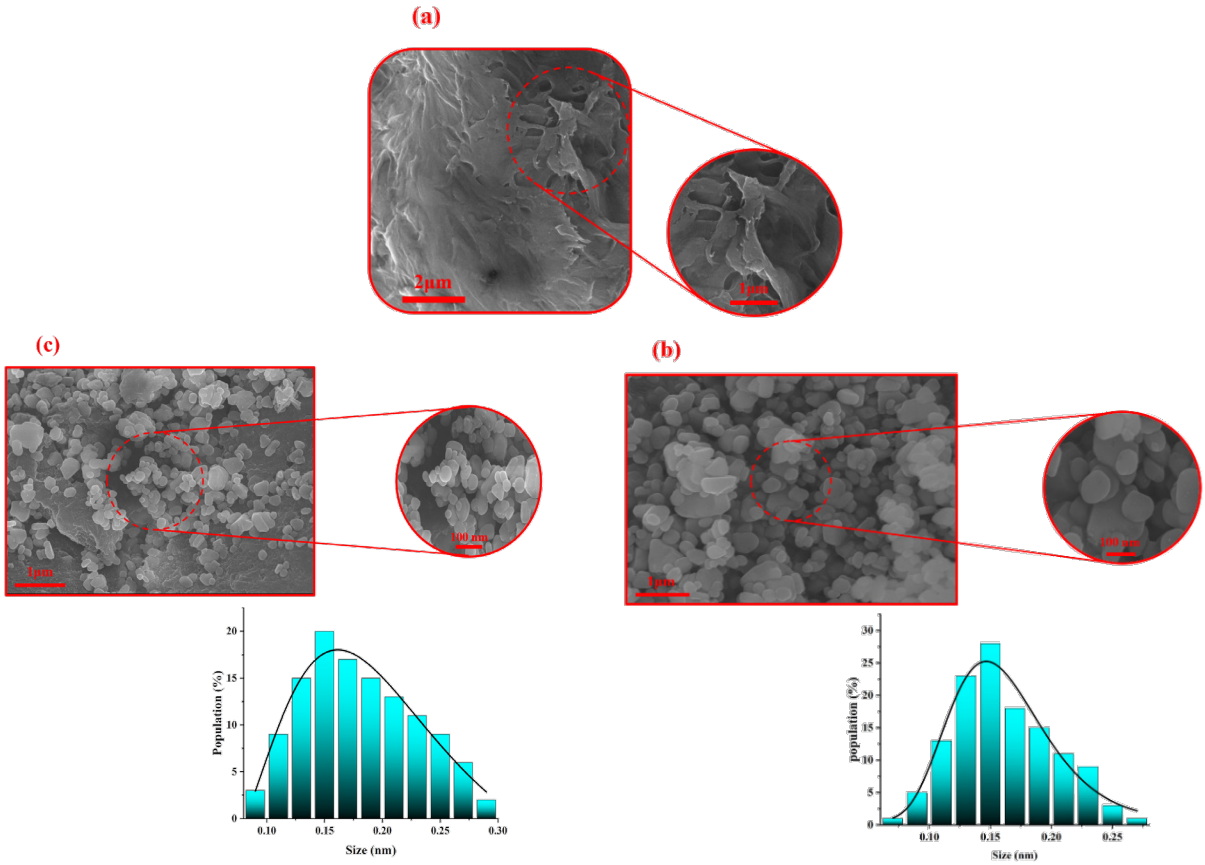

Figure 4. FESEM images of (a) CS, (b) ZnS NPs, and (c) ZnS/CS nanocomposite. Size distribution histograms with a log-normal fitting function are shown below for every FESEM.

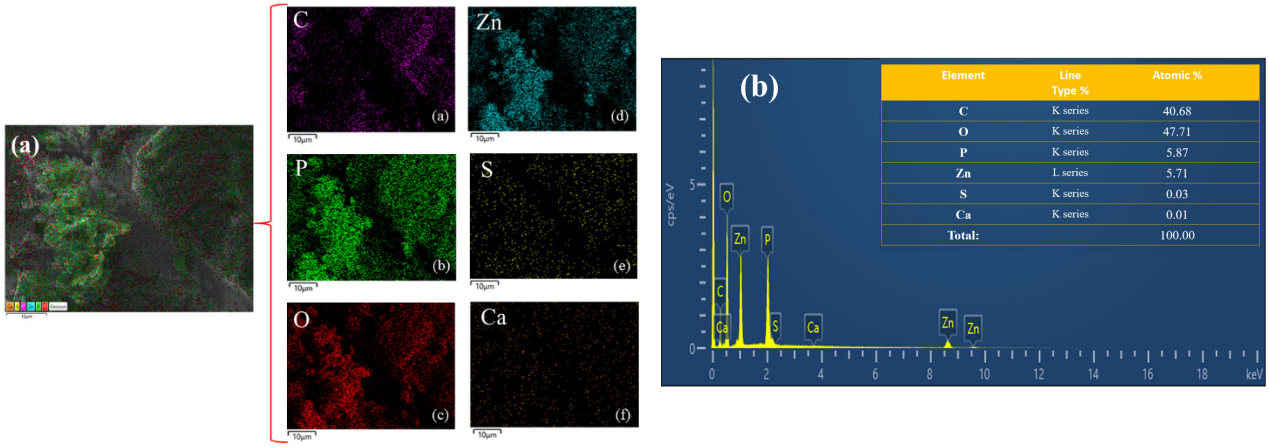

Figure 5. (a) elemental mapping of the prepared ZnS/CS nanocomposite (b) Elemental spectrum.

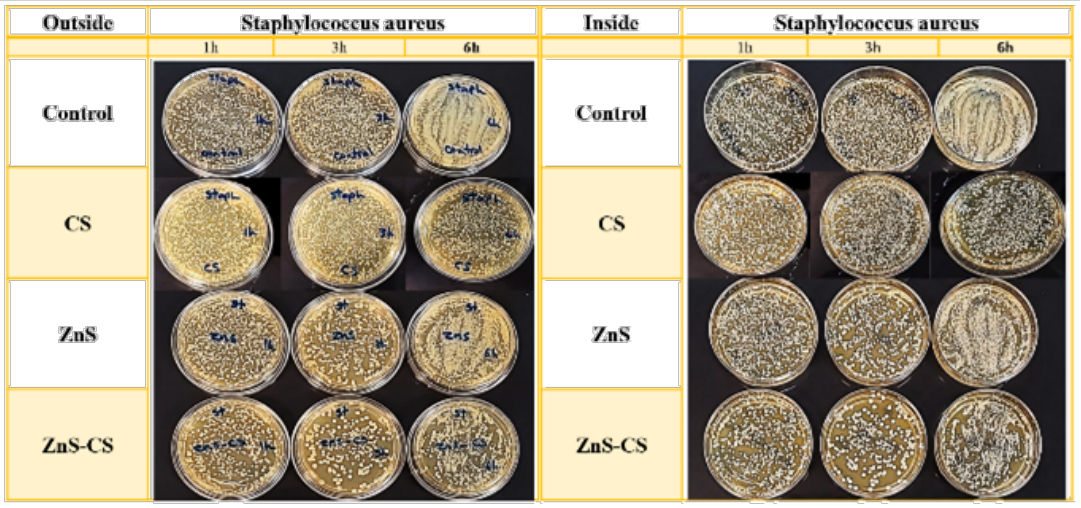

(a)

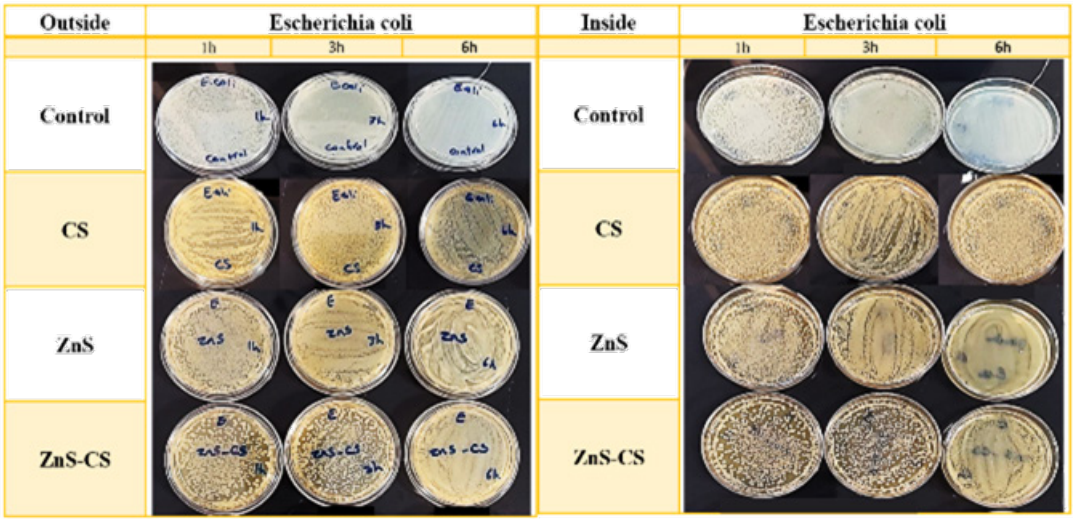

(b)

Figure 6. Antibacterial activity of pure CS, ZnS NPs, and ZnS/CS nanocomposite via standard colony counting assay against E. coli and S. aureus bacteria.

TABLE 4. Reduction in colony forming unit (%) for CS, ZnS NPs, and ZnS/CS nanocomposite.

Time	S. aureus (ATCC 25923)					E. coli (ATCC 25922)				
	Item	Blank	CS	ZnS	ZnS-CS	Item	Blank	CS	ZnS	ZnS-CS
1h	Viable count (CFU/ml)	1×10^6	$>9.5\times10^5$	$>9.5\times10^5$	9×10^5	Viable count (CFU/ml)	1×10^6	$>9.5\times10^5$	$>9.5\times10^5$	8×10^5
	Reduction Percentage (%)	-	<5%	<5%	10	Reduction Percentage (%)	-	<5%	<5%	20
3h	Viable count (CFU/ml)	1×10^6	$>9.5\times10^5$	6×10^5	4×10^5	Viable count (CFU/ml)	1×10^6	$>9.5\times10^5$	$>9.5\times10^5$	8×10^5
	Reduction Percentage (%)	-	<5%	40	60	Reduction Percentage (%)	-	<5%	<5%	20
6h	Viable count (CFU/ml)	1×10^6	$>9.5\times10^5$	6×10^5	4×10^5	Viable count (CFU/ml)	1×10^6	$>9.5\times10^5$	$>9.5\times10^5$	8×10^5
	Reduction Percentage (%)	-	<5%	40	60	Reduction Percentage (%)	-	<5%	<5%	20

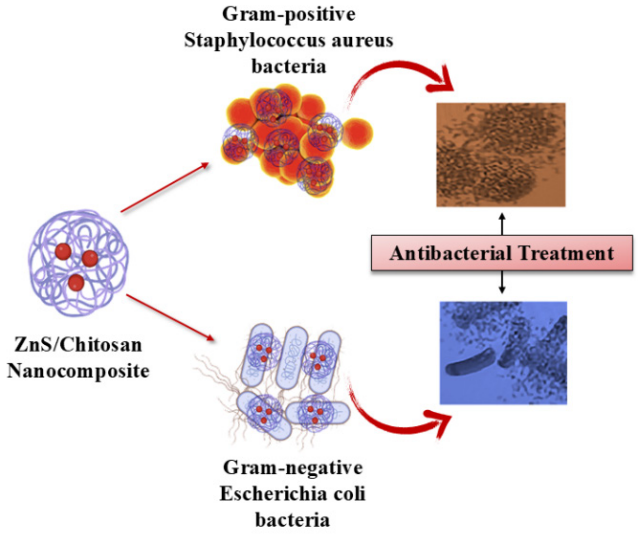

Figure 7. Antibacterial mechanism of action of ZnS/Chitosan nanocomposite.

4. CONCLUSION

ZnS nanoparticles as well as a ZnS/Chitosan hybrid were successfully synthesized using a straightforward chemical co-precipitation technique. The average size of the synthesized ZnS and ZnS/chitosan ranged from 30 to 40 nanometers. These findings were validated through XRD, FESEM, and FTIR analyses.

FTIR analysis revealed that every single one of the samples had stretching vibrations of the following types: O-H, C-H, C=O, C-N, and Zn-S. The material was investigated to examine its ability to eradicate both Gram-positive and Gram-negative bacteria. When it came to eliminating germs, it was discovered that the ZnS/Chitosan combo was more successful than both pure ZnS and CS. This suggests its potential applicability for antimicrobial purposes.

ACKNOWLEDGEMENTS

The authors wish to acknowledge Semnan University for the all support throughout this work.

REFERENCES

1. Aboelwafa, M. A., Abdelghany, A. M., & Meikhail, M. S. (2021). Preparation, characterization, and antibacterial activity of ZnS-NP's filled polyvinylpyrrolidone/chitosan thin films. *Biointerf. Res. Appl. Chem*, *11*(6), 14336-14343. http://dx.doi.org/10.33263/BRIAC116.1433614343
2. Afzali, A. H., Hajiebrahimi, M., Hosseinieh Farahani, M. M., Alamdari, S., & Mirzaee, O. (2024). Exploring the Potential of ZnS/CdS Dual Nanocomposites in Photocatalytic Degradation for Water Cleanup. *Advanced Ceramics Progress*, *10*(4), 5-14. https://doi.org/10.30501/acp.2025.486343.1165
3. Alamdari, S., Haji Ebrahimi, M., Mirzaee, O., Jafar Tafreshi, M., Majlesara, M. H., Tajally, M., ... & Mohammadi, A. (2022). Cerium doped tungsten-based compounds for thermoluminescence application. *Progress in Physics of Applied Materials*, *2*(1), 35-40. https://doi.org/10.22075/ppam.2022.27086.1028
4. Alamdari, S., Hemmati, M., Jafar Tafreshi, M., & Ehsani, M. H. (2023). Erbium doped Barium Tungstate-Chitosan Nanocomposite: Luminescent Properties. *Progress in Physics of Applied Materials*, *3*(2), 119-123. https://doi.org/10.22075/ppam.2023.31808.1065
5. Alamdari, S., Mirzaee, O., Jahroodi, F. N., Tafreshi, M. J., Ghamsari, M. S., Shik, S. S., ... & Park, H. H. (2022). Green synthesis of multifunctional ZnO/chitosan nanocomposite film using wild Mentha pulegium extract for packaging applications. *Surfaces and Interfaces*, *34*, 102349. https://doi.org/10.1016/j.surfin.2022.102349
6. Ali, Z. I., Mosallam, F. M., Sokary, R., Afify, T. A., & Bekhit, M. (2021). Radiation synthesis of ZnS/chitosan nanocomposites and its anti-bacterial activity. *International Journal of Environmental Analytical Chemistry*, *101*(3), 379-390. https://doi.org/10.1080/03067319.2019.1667986
7. Almadari, S., Mansoorian, M., & Mousavi-Kamazani, M. (2025). Biosafe Chitosan Films Reinforced with Zinc Oxide/Graphene Oxide: Comprehensive Multifunctional Properties. *BioNanoScience*, *15*(1), 1-14. https://doi.org/10.1007/s12668-025-01808-7
8. Ameh, T., Zarzosa, K., Dickinson, J., Braswell, W. E., & Sayes, C. M. (2023). Nanoparticle surface stabilizing agents influence antibacterial action. *Frontiers in Microbiology*, *14*, 1119550. https://doi.org/10.3389/fmicb.2023.1119550
9. Aqeel, M., Ikram, M., Asghar, A., Haider, A., Ul-Hamid, A., Naz, M., ... & Ali, S. (2020). Synthesis of capped Cr-doped ZnS nanoparticles with improved bactericidal and catalytic properties to treat polluted water. *Applied Nanoscience*, *10*, 2045-2055. https://doi.org/10.1007/s13204-020-01268-3
10. Badabagni, P. R., & Nayakanti, D. (2023) Zn-based Nanomaterials for Antimicrobial Applications: A Short Review. https://doi.org/10.22214/ijraset.2023.49817
11. Budea, C. M., Pricop, M., Mot, I. C., Horhat, F. G., Hemaswini, K., Akshay, R., ... & Marincu, I. (2023). The Assessment of Antimicrobial Resistance in Gram-Negative and Gram-Positive Infective Endocarditis: A Multicentric Retrospective Analysis. *Medicina*, *59*(3), 457. https://doi.org/10.3390/medicina59030457

12. Carstens, N., Mirigliano, M., Strunskus, T., Faupel, F., Lupan, O., Milani, P., & Vahl, A. (2021). Nanoparticles as Building Units for Bio-Inspired Electronics–Switching and Sensing. In *Electronics, Communications and Computing* (pp. 88-93). https://doi.org/10.52326/ic-ecco.2021/EL.01

13. Duwarah, H., Devi, J., Sharma, N., Saikia, K. K., & Datta, P. (2023). Zinc Sulphide Quantum Dots' Applications in Antibacterial as well as Estimation of E. coli Concentration by Fabricating Mem-Mode Devices. *Advanced Materials Research*, *1176*, 11-18. https://doi.org/10.4028/p-5m1d1m

14. Farahani, M. M. H., Hajiebrahimi, M., Alamdari, S., Najafzadehkhoee, A., Khounsaraki, G. M., Agheb, M., ... & Mirzaee, O. (2024). Synthesis and antibacterial activity of silver doped zinc sulfide/chitosan bionanocomposites: A new frontier in biomedical applications. *International Journal of Biological Macromolecules*, *280*, 135934. https://doi.org/10.1016/j.ijbiomac.2024.135934

15. Frieri, M., Kumar, K., & Boutin, A. (2017). Antibiotic resistance. *Journal of infection and public health*, *10*(4), 369-378. https://doi.org/10.1016/j.jiph.2016.08.007

16. Hajiebrahimi, M., Alamdari, S., & Mirzaee, O. (2024). The Potential of Silver-Doped Zinc Sulfide/Cadmium Sulfide Nanocomposites in Optoelectronic Applications. *Iranian Journal of Materials Science & Engineering*, *21*(4). http://dx.doi.org/10.22068/ijmse.3784

17. Hajiebrahimi, M., Alamdari, S., Mirzaee, O., & Tajally, M. (2022). Luminescence investigation of Ce doped ZnO/$CdWO_4$ nanocomposite. *Advanced Ceramics Progress*, *8*(3), 8-12. https://doi.org/10.30501/acp.2022.363264.1102.

18. Hajiebrahimi, M., Alamdari, S., Mirzaee, O., Albov, D., & Hvizdos, P. (2025). Flexible cerium-doped tungstate oxide/titanium dioxide nanocomposite for high-sensitivity energy conversion in optical applications. *Journal of Materials Science: Materials in Electronics*, *36*(2), 103. https://doi.org/10.1007/s10854-024-14141-8

19. Hassan, S. A. (2020). Artificial neural networks for the inverse design of nanoparticles with preferential nano-bio behaviors. *The Journal of Chemical Physics*, *153*(5). https://doi.org/10.1063/5.0013990

20. Kang, S. G., Lee, K. E., Singh, M., & Vinayagam, R. (2023). Salicylic-zinc nanocomposites with enhanced antibacterial activity. *Coatings*, *13*(5), 941. https://doi.org/10.3390/coatings13050941

21. Khoerunnisa, F., Nurhayati, M., Herlini, H., Adzkia, Q. A. A., Dara, F., Hendrawan, H., ... & Lim, J. (2023). Design and application of chitosan-CuO nanocomposites synthesized via novel hybrid ionic gelation-ultrasonication methods for water disinfection. *Journal of Water Process Engineering*, *52*, 103556. https://doi.org/10.1016/j.jwpe.2023.103556

22. Kusrini, E., Wilson, L. D., Padmosoedarso, K. M., Mawarni, D. P., Sufyan, M., & Usman, A. (2023). Synthesis of Chitosan Capped Zinc Sulphide Nanoparticle Composites as an Antibacterial Agent for Liquid Handwash Disinfectant Applications. *Journal of Composites Science*, *7*(2), 52. https://doi.org/10.3390/jcs7020052

23. Mekuye, B., & Abera, B. (2023). Nanomaterials: An overview of synthesis, classification, characterization, and applications. *Nano Select*, *4*(8), 486-501. https://doi.org/10.1002/nano.202300038

24. Moradi, D., Hosseini, M., Hajiebrahimi, M., Alamdari, S., & Mirzaee, O. (2024). Optical Properties of Flexible Nanocomposites Synthesized as Powders via the Hydrothermal Method Under Ionizing Excitations. *Advanced Ceramics Progress*, *10*(3), 15-22. https://doi.org/10.30501/acp.2024.486443.1166

25. Mustafa, H. N., & Al-Ogaidi, I. (2023). Efficacy of zinc sulfide-chitosan nanoparticles against bacterial diabetic wound infection. *Iraqi journal of agricultural sciences*, *54*(1), 1-17. https://doi.org/10.36103/ijas.v54i1.1671

26. Paula, A. J., & Koo, H. (2017). Nanosized building blocks for customizing novel antibiofilm approaches. *Journal of Dental Research*, *96*(2), 128-136. https://doi.org/10.1177/0022034516679397

27. Pires, J. R. A., Rodrigues, C., Coelhoso, I., Fernando, A. L., & Souza, V. G. L. (2023). Current applications of bionanocomposites in food processing and packaging. *Polymers*, *15*(10), 2336. https://doi.org/10.3390/polym15102336

28. Singh, S. P., Singh, A. K., & Yadav, P. (2022). Synthesis and characterization of structural and optical properties of Ni-doped zinc sulfide nanoparticles. *Journal of Advanced Scientific Research*, *13*(04), 87-93. https://doi.org/10.55218/JASR.202213416

29. Valinezhad, N., Talebi, A. F., & Alamdari, S. (2023). Biosynthesize, physicochemical characterization and biological investigations of chitosan-Ferula gummosa essential oil (CS-FEO) nanocomposite. *International Journal of Biological Macromolecules*, *241*, 124503. https://doi.org/10.1016/j.ijbiomac.2023.124503

30. Zannat, K. E., Tanzim, S. M., Afrin, A., Saha, B. C., Joynal, J. B., Khanam, T. A., & Nira, N. H. (2023). Antibacterial Effects of Methanolic Leaf Extracts of Henna (Lawsonia inermis) Against Two Most Common Pathogenic Organisms: Gram Positive Staphylococcus aureus and Gram-Negative Escherichia coli. *Mymensingh medical journal: MMJ*, *32*(2), 296-302. https://pubmed.ncbi.nlm.nih.gov/37002737/